Journal of Zhejiang University SCIENCE A
ISSN 1673-565X (Print); ISSN 1862-1775 (Online)
www.zju.edu.cn/jzus; www.springerlink.com
E-mail: jzus@zju.edu.cn

Analysis and behaviour of FRP-confined short concrete columns subjected to eccentric loading

Xing-fei YUAN[†1,3], Shao-hua XIA[2], L. LAM[3], S.T. SMITH[4]

([1]*Department of Civil Engineering, Zhejiang University, Hangzhou 310027, China*)

([2]*School of Civil and Environmental Engineering, The University of Adelaide, Adelaide, SA 5005, Australia*)

([3]*Department of Civil and Structural Engineering, The Hong Kong Polytechnic University, Hong Kong, China*)

([4]*Department of Civil Engineering, Hong Kong University, Hong Kong, China*)

[†]E-mail: yuanxf@zju.edu.cn

Received June 29, 2007; revision accepted Sept. 20, 2007; published online Dec. 14, 2007

Abstract: Fibre-reinforced polymer (FRP) composites were widely utilized in civil engineering structures as the retrofit of reinforced concrete (RC) columns. To design FRP jackets safely and economically, the behaviour of such columns should be predicted first. This paper is concerned with the analysis and behaviour of FRP-confined RC circular and rectangular short columns subjected to eccentric loading. A simple design-oriented stress-strain model for FRP-confined concrete in a section analysis was first proposed. The accuracy was then proved by two test data. Following that, a parametric study including amount of FRP confinement, FRP strain capacity, unconfined concrete strength and shape of column section is provided. Some conclusions were obtained at the end of the paper. The work here will provide a comprehensive understanding of the behaviour of FRP-confined concrete columns. The simplicity of the model also enables a simple equivalent stress block to be developed for direct use in practical design.

Key words: Column, FRP confinement, Stress-strain model, Section analysis, Strength, Ductility
doi:10.1631/jzus.A071352 **Document code:** A **CLC number:** TU375

INTRODUCTION

One of the important applications of fibre-reinforced polymer (FRP) composites in civil engineering structures is the retrofit of reinforced concrete (RC) columns. In such application, an FRP jacket with the fibres oriented only or predominantly in the hoop direction is used to confine the concrete to enhance both the compressive strength and ultimate strain of the concrete. To achieve safe and economic designs of the FRP jackets, designers need to know and to have the means to predict the behaviour of such columns subjected to eccentric loading (Hadi, 2007). Provided that such columns are sufficiently stocky to be unaffected by slenderness, their behaviour and strength can be obtained from a section analysis based on a plane section assumption, provided that the stress-strain behaviour of FRP-confined concrete can be closely predicted.

Despite the simplicity of a section analysis, accurate results from such an analysis are of practical value in understanding the behaviour of such columns subjected to eccentric loading. As a result, the results from such a section analysis have been presented in a number of studies. Saadatmanesh *et al*.(1994) included a parametric study covering both circular and rectangular columns confined by wrapped FRPs. The behaviour of FRP-confined columns does not appear to have been accurately predicted in this study because of the use of Mander *et al*.(1988)'s model which has been shown to be inappropriate for FRP-confined concrete (Mirmiran and Singhvi, 2001). The studies of Monti *et al*.(2001) and Cheng *et al*.(2002) were on FRP-wrapped columns with the fibres predominantly in the hoop direction. Mirmiran *et al*.(2000) focused on concrete-filled FRP tubes which provide the re-

sistance in both axial and hoop directions. Stress-strain models for FRP-confined concrete developed by Samaan *et al*.(1998), Spoelstra and Monti (1999), Cheng *et al*.(2002), Harajli (2006), Youssef *et al*.(2007) were used in their own studies on the behaviour of FRP-confined concrete columns.

The present paper aims to obtain a comprehensive understanding of the behaviour of FRP-confined concrete columns by employing an accurate yet simple stress-strain model for FRP-confined concrete. The simplicity of the model also enables a simple equivalent stress block to be developed for direct use in practical design. Both circular and rectangular columns are covered in the study.

BEHAVIOUR AND STRESS-STRAIN MODEL FOR FRP-CONFINED CONCRETE

Extensive experimental studies have shown that FRP-confined concrete exhibits a monotonically ascending curve which is nearly bi-linear in shape if it is sufficiently confined. Otherwise, the stress-strain curve features a post-peak descending branch and the compressive strength is reached before FRP rupture. Lam and Teng (2003a) have suggested that the threshold value for a sufficient confinement is an actual confinement ratio not less than 0.07. The present study covers only the behaviour of FRP-confined short concrete columns with an actual confinement ratio exceeding 0.07.

Many stress-strain models have been proposed in the past few years for FRP-confined concrete. These models can be classified into two categories: (a) design-oriented models and (b) analysis-oriented models. For a comparison of most of these models, readers are referred to Lam and Teng (2003a), Teng *et al*.(2002), and de Lorenzis and Tepfers (2002a; 2002b). For retrofitting circular concrete columns using FRP jackets with fibres oriented only or predominantly in the hoop direction, Lam and Teng (2003a) proposed a simple yet accurate design-oriented model. This model is used in the present study for circular columns, together with an extension of it for the confinement of rectangular concrete columns with FRP as proposed by Lam and Teng (2003b).

The Lam and Teng (2003a)'s model is for sufficiently confined concrete. In this model, the stress-strain curves of the FRP-confined concrete are approximated using a parabolic first portion and a linear second portion. The compressive strength of FRP-confined circular concrete f'_{cc} for cases with $f_l / f'_{co} \geq 0.07$ can be predicted by

$$f'_{cc} / f'_{co} = 1 + 3.3 f_l / f'_{co}. \quad (1)$$

The ultimate strain of the FRP-confined circular concrete ε_{cu} is given by

$$\varepsilon_{cu} / \varepsilon_{co} = 1.75 + 12(f_l / f'_{co})(\varepsilon_{h,rup} / \varepsilon_{co})^{0.45}, \quad (2)$$

where ε_{co} is the axial strain at the compressive strain of the unconfined concrete, taken as 0.002, and $\varepsilon_{h,rup}$ is the FRP hoop rupture strain. In rectangular columns, external confinement by FRP is less effective than that in circular columns. Lam and Teng (2003b) suggested that the compressive strength and ultimate strain of the FRP-confined concrete can be predicted using Eqs.(1) and (2) with the introduction of shape factors. Consequently, Eqs.(1) and (2) become

$$f'_{cc} / f'_{co} = 1 + 3.3 k_{s1} f_l / f'_{co},, \quad (3)$$

$$\varepsilon_{cu} / \varepsilon_{co} = 1.75 + 12 k_{s2}(f_l / f'_{co})(\varepsilon_{h,rup} / \varepsilon_{co})^{0.45}, \quad (4)$$

where k_{s1} and k_{s2} are shape factors for strength and strain respectively. The detail definition can be found in Lam and Teng (2003b).

ANALYSIS OF FRP-CONFINED CIRCULAR AND RECTANGULAR SECTIONS

Basic assumptions

The analysis of the FRP-confined column sections using a suitable FRP-confined concrete stress-strain model is based on the following assumptions:

(1) Plane sections before deformation remain plane after deformation. Consequently, the strain at any point of the cross section is directly proportional to its perpendicular distance from the neutral axis.

(2) The FRP provides only lateral confinement, without any stiffness in the longitudinal direction.

(3) The stress-strain relationship of concrete in compression is defined by one of the available stress-strain models.

(4) The tensile strength of concrete is ignored.

(5) The steel reinforcing bars are elastic-perfectly plastic.

(6) Any confinement effect of steel hoop reinforcement is ignored.

(7) Compressive stresses and strains are taken as positive.

(8) The ultimate limit state is reached when the strain of the extreme compression fibre of concrete $\varepsilon_{c,max}$ attains the ultimate strain ε_{cu}.

Circular columns

Referring to a circular section shown in Fig.1, for a given depth of neutral axis d_n, the stress resultants of the compressive concrete at any loading stage, namely the axial force N_c and the bending moment about the reference axis going through the centre of the section M_c, can be found by integrating the stresses over the section:

$$N_c = \int_{D/2-d_n}^{D/2} \sigma_c b_c \mathrm{d}y\,, \tag{5}$$

$$M_c = \int_{D/2-d_n}^{D/2} \sigma_c b_c y \mathrm{d}y\,, \tag{6}$$

where b_c is the width of the section at a distance y from the reference axis (y>0 when above the reference axis and y<0 when below the reference axis).

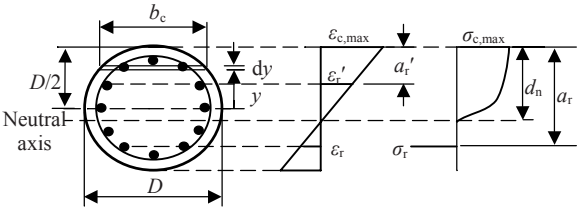

Fig.1 Strain and stress distributions over the circular section depth at the ultimate limit state

According to the plane section assumption, the strain of concrete at a distance y can be expressed as

$$\varepsilon_c = \frac{(y - y_n)}{d_n}\varepsilon_{c,max}\,, \tag{7}$$

where y_n=D/2−d_n. The stress-strain relationship of the FRP-confined concrete can then be rewritten as

$$\sigma_c = a(y - y_n)^2 + b(y - y_n) \quad \text{for } 0 \le \varepsilon_c \le \varepsilon_t\,, \tag{8a}$$

$$\sigma_c = c(y - y_n) + d \quad \text{for } \varepsilon_t \le \varepsilon_c \le \varepsilon_{cu}\,, \tag{8b}$$

where

$$a = -E_k \frac{\varepsilon_{c,max}^2}{d_n^2},\ b = E_c \frac{\varepsilon_{c,max}}{d_n},\ c = E_2 \frac{\varepsilon_{c,max}}{d_n},\ d = f_{co}'\,, \tag{9}$$

$$E_k = \frac{(E_c - E_2)^2}{4f_{co}'},\ \varepsilon_t = \frac{2f_{co}'}{(E_c - E_2)},\ E_2 = \frac{f_{cc}' - f_o}{\varepsilon_{cu}}. \tag{10}$$

For a column under an eccentric loading, integration of stresses over the cross section in Eqs.(5) and (6) can be carried out for three cases dependent on the maximum strain value of concrete and the location of the neutral axis.

(1) For $\varepsilon_{c,max}$>ε_t, and the location where ε_c=ε_t is within the cross section, that is 0<d_n<$D\varepsilon_{c,max}$/($\varepsilon_{c,max}$−ε_t), the axial force N_c and the bending moment M_c in Eqs.(5) and (6) become

$$N_c = \int_{\max(y_n,-D/2)}^{y_0} f_1 \mathrm{d}y + \int_{y_0}^{D/2} f_2 \mathrm{d}y\,, \tag{11}$$

$$M_c = \int_{\max(y_n,-D/2)}^{y_0} f_1 y \mathrm{d}y + \int_{y_0}^{D/2} f_2 y \mathrm{d}y\,, \tag{12}$$

where y_0 is the distance from the reference axis to the point where ε_c=ε_t in the strain profile of the cross section and can be expressed by

$$y_0 = D/2 - d_n((\varepsilon_{c,max} - \varepsilon_t)/\varepsilon_{c,max})\,, \tag{13}$$

$$f_1 = 2\sqrt{D^2/4 - y^2}\,[a(y - y_n)^2 + b(y - y_n)]\,, \tag{14}$$

$$f_2 = 2\sqrt{D^2/4 - y^2}\,[c(y - y_n) + d]\,. \tag{15}$$

(2) For $\varepsilon_{c,max}$>ε_t and the location where ε_c=ε_t falls outside the cross section, that is d_n≥$D\varepsilon_{c,max}$/($\varepsilon_{c,max}$−ε_t), Eqs.(5) and (6) can then be written as

$$N_c = \int_{-D/2}^{D/2} f_2 \mathrm{d}y\,, \tag{16}$$

$$M_c = \int_{-D/2}^{D/2} f_2 y \mathrm{d}y\,. \tag{17}$$

(3) For $\varepsilon_{c,max}$≤ε_t,

$$N_c = \int_{\max(y_n,-D/2)}^{y_0} f_1 \mathrm{d}y\,, \tag{18}$$

$$M_c = \int_{\max(y_n,-D/2)}^{y_0} f_1 y \mathrm{d}y\,. \tag{19}$$

The following general solutions can be applied for solving the integrals of Eqs.(5), (6), (11), (12) and (16)~(19).

$$\int_{y_1}^{y_2} \sqrt{R^2-y^2}\,\mathrm{d}y = \frac{1}{2}\left[y_2\sqrt{R^2-y_2^2} - y_1\sqrt{R^2-y_1^2} \right] + \frac{R^2}{2}\left[\arcsin\frac{y_2}{R} - \arcsin\frac{y_1}{R} \right], \tag{20}$$

$$\int_{y_1}^{y_2} \sqrt{R^2-y^2}\,y\mathrm{d}y = \frac{1}{3}[(R^2-y_1^2)^{3/2} - (R^2-y_2^2)^{3/2}], \tag{21}$$

$$\int_{y_1}^{y_2} \sqrt{R^2-y^2}\,y^2\mathrm{d}y = \frac{1}{8}\left[y_1(R^2-2y_1^2)\sqrt{R^2-y_1^2} - y_2(R^2-2y_2^2)\sqrt{R^2-y_2^2} \right] + \frac{R^4}{8}\left[\arcsin\frac{y_2}{R} - \arcsin\frac{y_1}{R} \right], \tag{22}$$

$$\int_{y_1}^{y_2} \sqrt{R^2-y^2}\,y^3\mathrm{d}y = \frac{1}{15}\sqrt{R^2-y_2^2}(-2R^4 - R^2y_2^2 + 3y_2^4) - \frac{1}{15}\sqrt{R^2-y_1^2}(-2R^4 - R^2y_1^2 + 3y_1^4). \tag{23}$$

Based on the strain profile in Fig.1, the strains in the reinforcing bars can be related to the strain at the extreme compression fibre of concrete $\varepsilon_{c,max}$ through

$$\varepsilon_r = \varepsilon_{c,max}((d_n - a_r)/d_n)\,, \tag{24}$$

$$\varepsilon_r' = \varepsilon_{c,max}((d_n - a_r')/d_n)\,, \tag{25}$$

where ε_r and ε_r' are the strains in reinforcing bars on the tension side and compression side respectively, and a_r and a_r' are the distances from the extreme concrete compression fibre to the centres of the reinforcing bars.

The stress resultants of the whole cross-section, namely the axial force N and the bending moment M about the reference axis, can then be written as

$$N = N_c + \sum_{j=1}^{n_r}(\sigma_{rj} - \sigma_{cj})A_{rj}\,, \tag{26}$$

$$M = M_c + \sum_{j=1}^{n_r}(\sigma_{rj} - \sigma_{cj})A_{rj}y_{rj}\,, \tag{27}$$

where n_r is the number of reinforcing bars, y_{rj} is the y coordinate of the centre of the jth reinforcing bar relative to the reference axis, σ_{rj} and σ_{cj} are the stresses of steel and concrete respectively at the centre of the jth reinforcing bar, with σ_{cj}=0 in the tension zone of concrete.

At the ultimate limit state, the axial force N, the bending moment M, and the depth of the neutral axis d_n can be taken as three basic parameters. Once one of them is known or M and N are related by a specified load eccentricity, the values of the two remaining parameters can be easily determined. Bending moment-axial load interaction curves can thus be easily generated.

The moment-curvature (M-ϕ) curves at a given axial load can be generated by specifying a sequence of suitable strain values for the extreme compression fibre of concrete $\varepsilon_{c,max}$ up to its ultimate value ε_{cu}. For each strain value, the neutral axis depth is varied until the resultant axial force acting on the section, calculated from Eq.(26), equals the applied axial load. Once the neutral axis position is determined, the moment can be evaluated and the curvature ϕ corresponding to the assumed strain $\varepsilon_{c,max}$ can be found by:

$$\phi = \varepsilon_{c,max}/d_n\,. \tag{28}$$

A computer program was developed based on the analysis procedures described above, and was used to generate the bending moment-axial load interaction curves and moment-curvature curves presented in this paper.

For stress-strain models that are expressed by a linear or quadratic function, the concrete stress-strain curve can be integrated over the compression zone to arrive at exact expressions for the integrals given in Eqs.(5), (6), (11), (12) and (16)~(19). For other models, numerical integration over the section is carried out by the layer (or the fibre element) method in which the column section is divided into many small horizontal layers.

Rectangular columns

The analysis of rectangular column sections is conducted using procedures similar to those described in Section 3.2 for circular columns, except that an equivalent stress block as shown in Fig.2 has been derived for rectangular sections based on Lam and

Teng (2003a)'s model. This stress block is characterized by two factors: the mean stress factor α and the compression force centroid factor γ, which are defined by

$$\alpha = \int_0^{\varepsilon_{c,max}} f_c \mathrm{d}\varepsilon_c / (f'_{co}\varepsilon_{c,max}), \tag{29}$$

$$\gamma = 1 - \int_0^{\varepsilon_{c,max}} f_c \varepsilon_c \mathrm{d}\varepsilon_c / (\varepsilon_{c,max} \int_0^{\varepsilon_{c,max}} f_c \mathrm{d}\varepsilon_c). \tag{30}$$

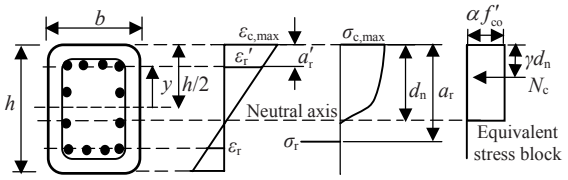

Fig.2 Strain and stress distributions over the rectangular section depth at the ultimate limit state

The expressions of these two factors can be easily derived using Lam and Teng (2003a)'s stress-strain model as given as follows.

(1) For $0 \le \varepsilon_{c,max} \le \varepsilon_t$,

$$\alpha = \frac{6E_c\varepsilon_{c,max}f'_{co} - (E_c - E_2)^2\varepsilon^2_{c,max}}{12f'^2_{co}}, \tag{31}$$

$$\gamma = 1 - \frac{16E_c\varepsilon_{c,max}f'_{co} - 3(E_c - E_2)^2\varepsilon^2_{c,max}}{24E_c\varepsilon_{c,max}f'_{co} - 4(E_c - E_2)^2\varepsilon^2_{c,max}}. \tag{32}$$

(2) For $\varepsilon_t \le \varepsilon_{c,max} \le \varepsilon_{cu}$,

$$\alpha = 1 + \frac{E_2\varepsilon_{c,max}}{2f'_{co}} - \frac{2f'_{co}}{3(E_c - E_2)\varepsilon_{c,max}}, \tag{33}$$

$$\gamma = 1 - [-2f'^3_{co} + 3f'_{co}\varepsilon^2_{c,max}(E_c - E_2)^2 + 2E_2\varepsilon^3_{c,max}(E_c - E_2)^2]/[-4f'^2_{co}\varepsilon_{c,max}(E_c - E_2) + 3E_2\varepsilon^3_{c,max}(E_c - E_2)^2 + 6f'_{co}\varepsilon^2_{c,max}(E_c - E_2)^2]. \tag{34}$$

The stress resultants of compressive concrete at any loading stage, namely the axial force N_c and the bending moment M_c about the reference axis which is located at the section mid-depth, can be found from:

$$N_c = \alpha f'_{co} b d_n, \tag{35}$$

$$M_c = (h/2 - d_n)\alpha f'_{co} b d_n. \tag{36}$$

The stress resultants of the whole cross-section (axial force N and bending moment M about the reference axis) can then be found using Eqs.(26) and (27).

COMPARISON WITH TEST DATA

The behaviour of the FRP-confined short concrete columns predicted by Lam and Teng (2003a)'s model is compared with the test data obtained by Saadatmanesh *et al*.(1996) and by Xiao *et al*.(1999) on FRP-confined circular RC columns. Though the test by Xiao *et al*.(1999) was aimed to analyse the retrofit effectiveness of FRP-confined columns on shear strength, it is suitable to be compared in this analysis because no shear failure occurred during the test.

Comparison with columns tested by Saadatmanesh *et al*.(1996)

The results of two FRP-confined cantilever circular RC columns tested by Saadatmanesh *et al*.(1996) are first used to compare with the predictions from the section analysis. These two columns had a diameter of 305 mm and a total height of 2410 mm (including a 381 mm high by 1067 mm wide and 914 mm deep base, as well as a thickened column top of 406 mm width and height) and were reinforced longitudinally with 14 equally spaced steel bars having a diameter of 12.7 mm and yield strength of 358 MPa. The transverse reinforcement was provided by steel wire hoops of 3.5 mm diameter with a spacing of 89 mm and yield strength of 301 MPa. The clear concrete cover from the concrete surface to the outside of the hoop steel was 10 mm. A difference between these two columns is in the details of the anchorage of longitudinal reinforcement bars. For the column labelled as C-2, the longitudinal reinforcement bars were lap-spliced with the starter bars from the footing (lap-spliced bars). For another column labelled as C-5, the longitudinal reinforcement bars were anchored into the footing using standard 90° hooks (continuous bars). Both columns were wrapped with five layers of glass (FRP) straps of 0.8 mm per layer thickness producing a total thickness of GFRP of 4.8 mm. The GFRP was applied to the potential plastic hinge zone and provided passive confinement to the columns. In testing, the columns were subjected to a constant axial load of 445 kN and a reversed lateral cyclic load with

a shear span of 1801 mm. The measured concrete strength was 38.3 MPa for the column with lap-spliced bars and 36.5 MPa for the column with continuous bars. It was not made evident by Saadatmanesh *et al*.(1996)'s test if these were compressive cube or cylinder concrete strengths. The compressive strength of the unconfined concrete f_{co}' is therefore taken as being directly equal to the tested strengths, i.e. f_{co}'=38.3 MPa and 36.5 MPa for columns C-2 and C-5 respectively. The GFRP straps had an elastic modulus of 18600 MPa and the ultimate hoop strain of the GFRP was taken as 1.6%. Monti *et al*.(2001) used such a strain when using one of these two Saadatmanesh *et al*.(1996)'s columns in their comparison with results from their predicted stress-strain model for FRP confined column. Both of Saadatmanesh *et al*.(1996)'s columns used in the current study were sufficiently confined having a confinement ratio of f_l/f_{co}'=0.245 for the column with lap-spliced bars (specimen C-2) and 0.257 for the column with continuous bars (specimen C-5).

Figs.3 and 4 show comparisons between the load-displacement curves and the load-displacement ductility ratio curves predicted from the section analysis for monotonic loading and the envelopes of the hysteresis loops obtained from the tests respectively. The displacement ductility ratio μ_Δ was originally expressed by Seible *et al*.(1997) as

$$\mu_\Delta = \frac{\Delta}{\Delta_y} = 1 + 3\left(\frac{\phi}{\phi_y} - 1\right)\frac{L_p}{L}\left(1 - 0.5\frac{L_p}{L}\right), \quad (37)$$

where ϕ_y is the curvature at the first yield that can be determined from a sectional moment-curvature analysis, Δ and Δ_y are the displacements corresponding to the curvatures ϕ and ϕ_y respectively. The shear span is denoted by L, and L_p is the length of the plastic hinge zone given by Seible *et al*.(1997) as

$$L_p = 0.08L + 0.022 f_{sy} d_b, \quad (38)$$

where f_{sy} and d_b are the yield strength and diameter of the longitudinal steel reinforcing bars respectively.

Figs.3 and 4 show that both the load-displacement curves and the load-displacement ductility ratio curves obtained from the section analysis using Lam and Teng (2003a)'s stress-strain model match well with Saadatmanesh *et al*.(1996)'s tests. It is also noted that, after the hoop effect of the CFRP was activated, the test load was slightly larger than those from the prediction, which might be caused by the ignorance of the hoop effect of the transverse reinforcement in the prediction. In addition, the an-

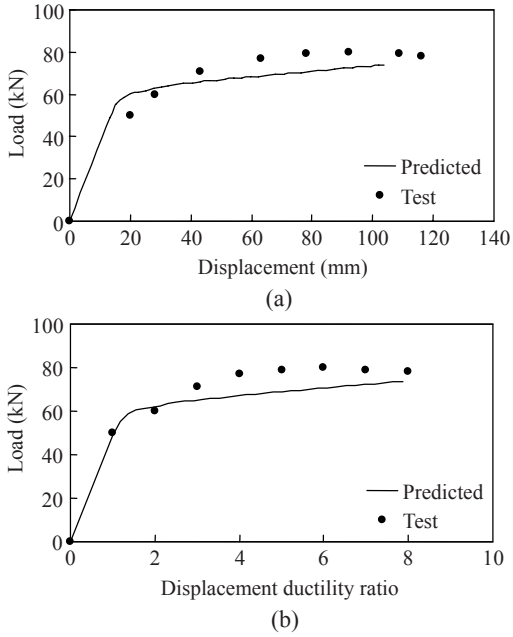

Fig.3 Comparison of test and predicted result for column C-2 of Saadatmanesh *et al*.(1996). (a) Load-displacement curve; (b) Load-displacement ductility ratio curve

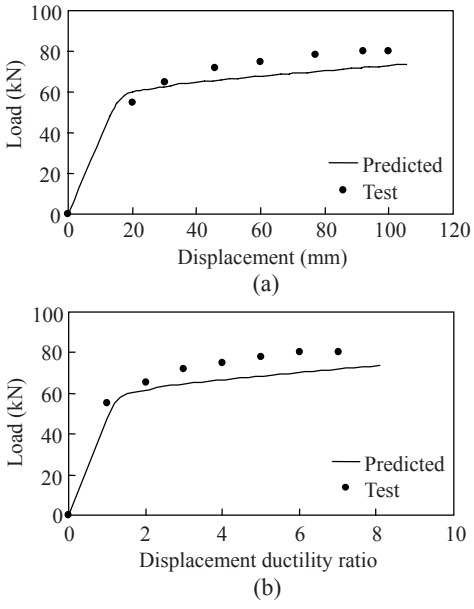

Fig.4 Comparison of test and predicted result for column C-5 of Saadatmanesh *et al*.(1996). (a) Load-displacement curve; (b) Load-displacement ductility ratio curve

chorage of the longitudinal steel reinforcing bars does not appear to be an issue because good correlation was observed between the experimental results and analytical predictions.

Comparison with columns tested by Xiao *et al.*(1999)

The circular columns tested by Xiao *et al*.(1999) had a diameter of 610 mm and a height of 2440 mm (excluding a 450 mm thick base from each end), and a column labeled by Xiao *et al*.(1999) as CS-CSJ-RT is used in this section. The column was reinforced with 20 deformed No.19 steel bars having a nominal diameter of 19.1 mm and yield strength of 303 MPa. The cover from the concrete surface to the outside of the hoop steel was 25 mm, with the hoop steel diameter equal to 6.4 mm and spaced at 150 mm centres. The columns were tested under cyclic shear in double curvature with a constant axial compressive load of 665 kN. The concrete cylinder compressive strength was 37.1 MPa and the column was wrapped with three continuous layers of GFRP having a single layer thickness of 2.54 mm near the ends of the column. Two layers of GFRP were applied to the middle portion of the column but the ends of the column, being more critical region due to higher bending moment, which were wrapped with three layers of GFRP are used for all subsequent calculations. The elastic modulus and ultimate strength of the GFRP were 38000 and 552 MPa respectively. Since the actual hoop strain of the GFRP at the ultimate state of the columns was not provided in Xiao *et al*.(1999)'s study, both 50% and 60% of the material tensile strength for hoop rupture is used in the present study, since the average tensile strength at hoop rupture from the database of the FRP confined concrete columns was reported by Teng *et al.*(2002) to be about 59% of the material tensile strength for CFRP. The compressive strength of the unconfined concrete f_{co}' is taken as 85% of the concrete cylinder compressive strength (i.e. f_{co}'=0.85×37.1=31.5 MPa) as this gave the best correlation with test results. The column therefore had a confinement ratio of f_l/f_{co}'=0.219 and 0.262 for 50% and 60% of the material tensile strength respectively.

Comparisons between the load-displacement curves and the load-displacement ductility ratio curves predicted by the section analysis for the monotonic loading and the envelopes of the hysteresis loops obtained from the tests are shown in Fig.5. It can be seen that the curves obtained by taking the hoop strain of the GFRP at the ultimate to be 60% of the material strength correlated well with those from the experiment for both the displacement and displacement ductility ratio. The FRP properties of E_{frp} and $\varepsilon_{h,rup}$ are important in the prediction of the behaviour of FRP-confined columns, but more detailed studies about the effects of the properties of FRP at hoop rupture will be discussed in the following section. Concrete strength and section shape are other two important parameters and these will also be discussed in the following section.

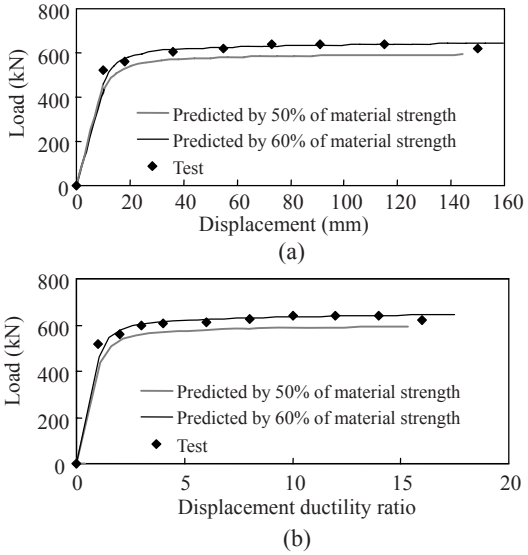

Fig.5 Comparison of test and predicted result for column CS-CSJ-RT of Xiao *et al.*(1999). (a) Load-displacement curve; (b) Load-displacement ductility ratio curve

From the comparisons with Saadatmanesh *et al*.(1996)'s and Xiao *et al*.(1999)'s tests, it can be concluded that the proposed model gives a satisfactory prediction of the behaviour of the circular column confined with FRP jackets and therefore can be used for assessing the retrofit effectiveness of such columns.

PARAMETRIC STUDY USING LAM AND TENG'S MODEL

General

This section presents the results of a parametric

study using the procedures described in Section 3 based on Lam and Teng's models (Lam and Teng, 2003a; 2003b; Teng *et al.*, 2002) for both circular and rectangular FRP-confined columns. The circular column section described in Section 4.1, which has an unconfined concrete strength of f_{co}'=20.1 MPa and wrapped with five layers of CFRP will still be used as the reference column. Parameters studied include the amount and strain capacity of FRP, unconfined concrete strength, and the shape of column section. The axial strength N_u, moment capacity M_u, curvature ϕ and curvature ductility factor u_ϕ of the confined columns with the effects of the above parameters will be investigated. In addition to displacement ductility as used by Saadatmanesh *et al.*(1994), curvature ductility is also a widely used means to denote ductility, defined as follows, and will be used herein:

$$\mu_\phi = \phi / \phi_y , \tag{39}$$

where ϕ_y is the curvature at first yield.

In presenting the results, the axial strength and moment capacity will be given as normalized values N_u/N_{uo} and M_u/M_{uo} for circular columns (Figs.6~8), due to constant values of N_{uo} and M_{uo}. Note that the axial strength and moment capacity of the unconfined columns with the same unconfined concrete strength in pure compression and pure bending, are denoted by N_{uo} and M_{uo} respectively. For comparison of shape of column section (Fig.9), the axial strength N_u and moment capacity M_u will be given as absolute and not divided by N_{uo} and M_{uo} as the latter vary depending on the column shape.

Amount of FRP confinement

Fig.6 shows the effect of the amount of the FRP on the predicted behaviour of RC circular columns, where the reference column is compared with an unconfined column and a column wrapped with 10 layers of CFRP, both having the same unconfined concrete strength f_{co}' as the reference column. The unconfined column possesses N_{uo} of 8274 kN and M_{uo} of 558 kN·m. It can be seen from Fig.6 that an increase in the amount of FRP results in substantial increases in the strength and ductility of the columns. Compared to the unconfined column, an increase of 66% in axial strength is found for the reference column with the five-layer CFRP jacket under pure compression, and this increase is nearly double (131%) for the ten-layer CFRP jacket (Fig.6a). Much higher increases in curvature and ductility are found from the FRP confinement (Fig.6b). In the case of pure bending (i.e. when N_u/N_{uo}=0), the curvature ductility factor is only about 3 for the unconfined column, but considerably increases to approximately 20 and 40 for the columns confined by the five-layer and ten-layer FRP respectively (Fig.6c). Note that if the axial load is near zero, the FRP confinement results in little enhancement in the moment capacity. This indicates that in the case of pure bending, FRP jackets with fibres oriented only in the hoop direction will provide minimal enhancement to the moment capacity. If the moment capacity is to be enhanced,

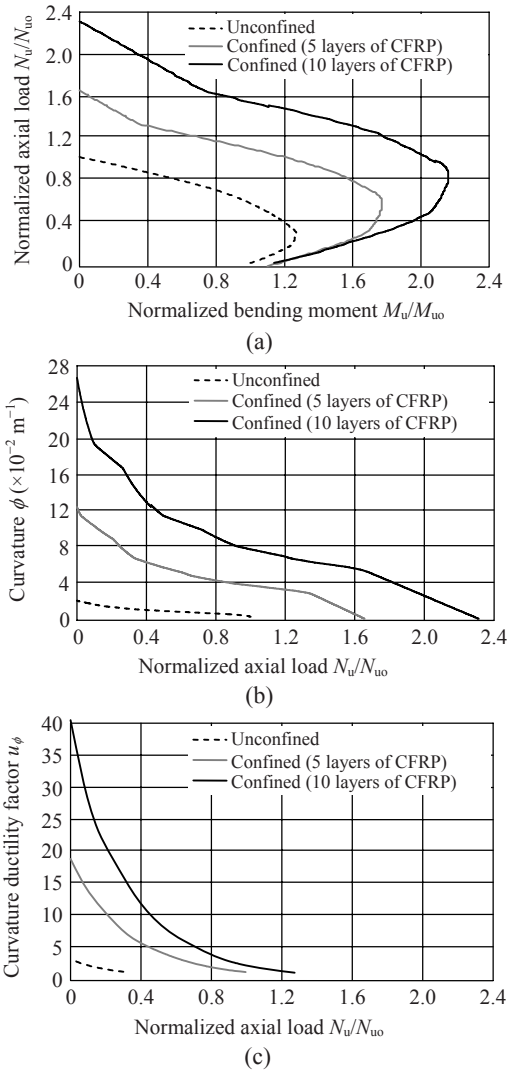

Fig.6 Effect of the amount of FRP confinement on column behaviour. (a) Strength; (b) Curvature; (c) Ductility

the recourse to FRP jackets with fibres orientated in the longitudinal direction of the column will have to be made.

FRP strain capacity

Fig.7 shows the effect of the FRP strain capacity on the predicted behaviour of columns, where the reference column (CFRP confined) is compared with an unconfined column and an aramid FRP (AFRP) confined column with the same unconfined concrete strength. The elastic modulus and hoop rupture strength of the AFRP are 125000 MPa and 1800 MPa respectively, and the total thickness of the AFRP wrap is 0.9917 mm. Such an AFRP wrap supplies the same maximum confining pressure to the column as the five-layer CFRP wrap, but has a higher strain capacity. The strain of the AFRP at hoop rupture is 0.0144, while that of the CFRP is 0.00913. According to Eq.(8) the ultimate axial strain of the FRP-confined concrete column wrapped with the AFRP is 18.2% higher than that of the reference column wrapped with CFRP. While this increase in the ultimate strain of the confined concrete has no effect on the axial strength and moment capacity of the columns (Fig.7a), it results in considerable increases in the curvature and ductility factor (Figs.7b and 7c). At an axial load of 5000 kN,

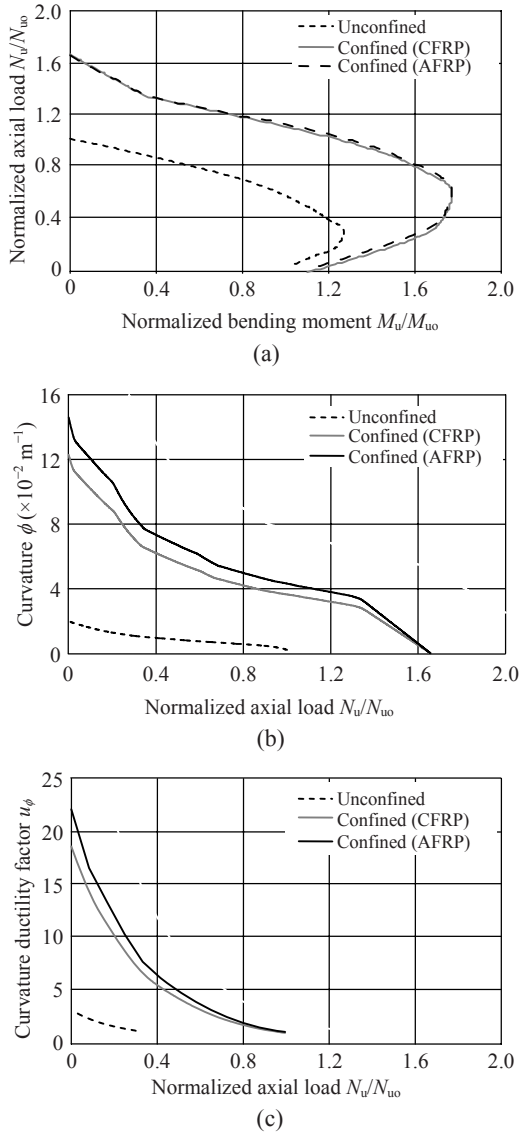

Fig.7 Effect of FRP strain capacity on column behaviour. (a) Strength; (b) Curvature; (c) Ductility

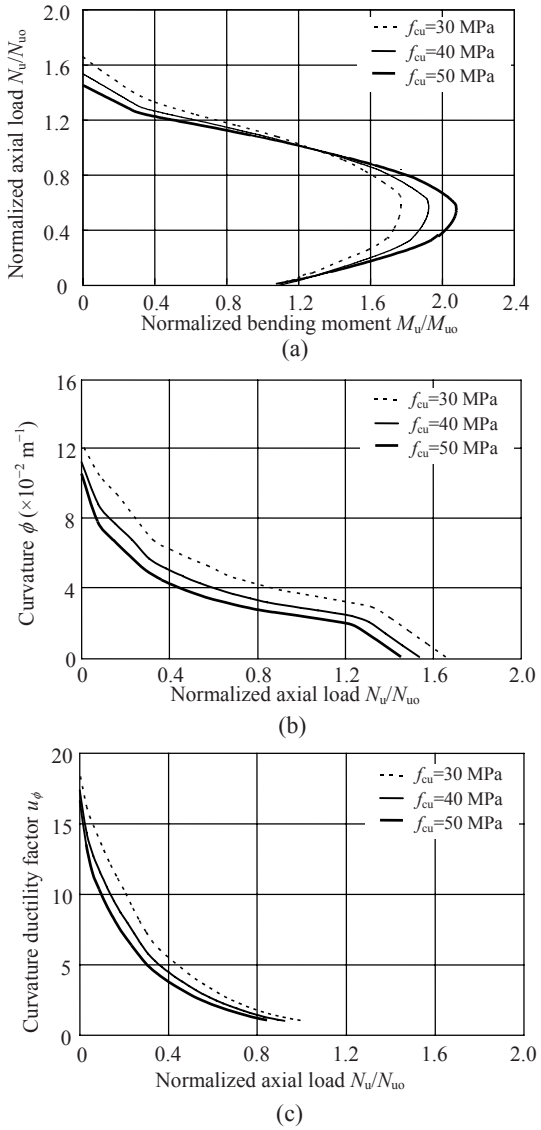

Fig.8 Effect of unconfined concrete strength on column behaviour. (a) Strength; (b) Curvature; (c) Ductility

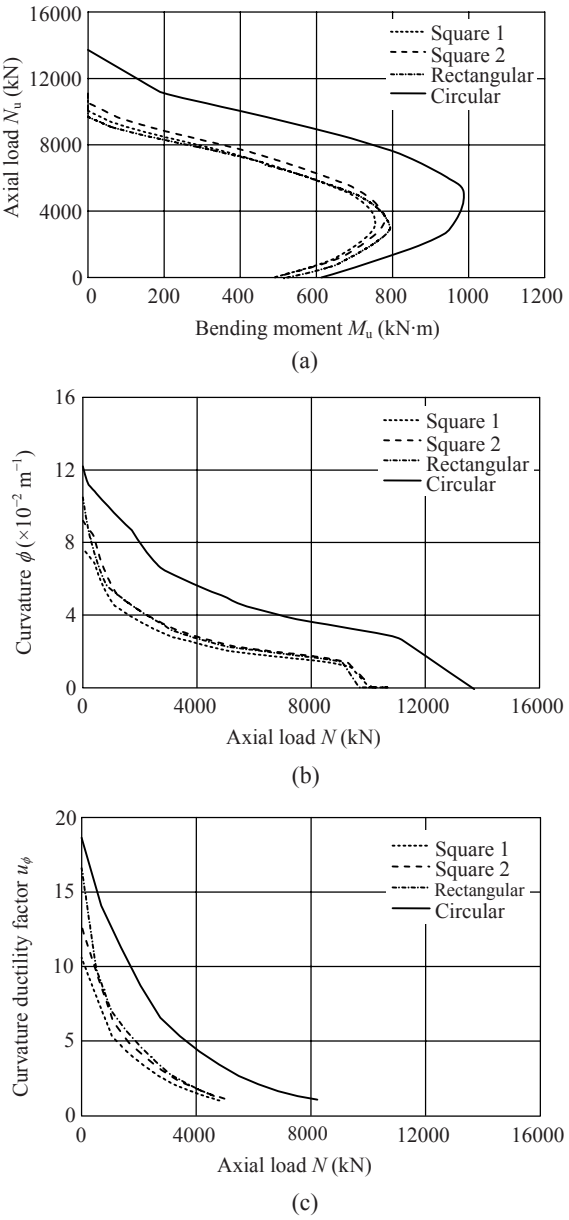

Fig.9 Effect of column shape on column behaviour. (a) Strength; (b) Curvature; (c) Ductility

the ultimate curvature and curvature ductility factor of the column are 19% and 18% higher respectively for the column confined by the AFRP than those for the one confined by the CFRP. This observation confirms that the ductility of the column is closely related to the strain capacity of the confining FRP.

Unconfined concrete strength

Fig.8 shows the effect of the unconfined concrete strength on the behaviour of the confined columns. The reference column that has a concrete cube compressive strength f_{cu} of 30 MPa (f_{co}'=20.1 MPa) is compared with two columns which are wrapped with the same amount of the CFRP (five layers) but have the cube concrete compressive strengths of 40 MPa and 50 MPa, corresponding to unconfined concrete strengths of f_{co}'=26.8 MPa and 33.5 MPa respectively. The corresponding two unconfined columns have axial strengths in pure compression of 10129 kN and 11984 kN, and pure bending moment capacity of 575 kN·m and 588 kN·m respectively. It is interesting to note from Fig.8a that at a load level higher than the axial strength (8274 kN) of the corresponding unconfined column, an increase in the unconfined concrete strength has a negative effect on the normalized moment capacity, but at a load level below the axial strength of the corresponding unconfined column, the effect is inversed. On the other hand, the column with a higher unconfined concrete strength is seen to be less ductile (Figs.8b and 8c). This is because the ductility of the confined column is closely related to the ultimate strain of confined concrete, and also the ultimate strain of the confined concrete is highly dependent on the confinement ratio. An increase in the unconfined concrete strength without increasing the amount of the FRP results in a reduced confinement ratio which negatively affects the ultimate strain of the confined concrete. This observation suggests that although an improvement in the axial strength of columns can be achieved by using higher strength concrete, there will be no corresponding improvement in the ductility.

Shape of column section

The rectangular columns used for demonstrating the effect of section shape have the same cross sectional area and internal reinforcement ratio as the reference circular column defined in Section 4.1. Three rectangular columns are defined, which consist of two square columns with corner radius R_c of 30 and 60 mm respectively, and a rectangular column with an aspect ratio of h/b=1.25 and a corner radius of 60 mm. These three rectangular columns are wrapped with the CFRP with the same volumetric ratio as the reference column that is wrapped with five layers of the CFRP with a total thickness of 0.85 mm. The FRP thicknesses on the rectangular columns are different because of the difference in the length of circumference.

The distance from the concrete surface to the centre of the steel bars is 50 mm, which is the same as the reference circular column. The details of the rectangular columns and the reference circular column are given in Table 1.

Table 1 Detailed information of rectangular, square and circular columns

Column	b (mm)	h (mm)	t (mm)	f_{cu} (MPa)	f_{co}' (MPa)	k_{s1}	k_{s2}	f_l'/f_{co}'
Square 1	532	532	0.7525	30	20.1	0.460	0.460	0.209
Square 2	532	532	0.7525	30	20.1	0.585	0.585	0.209
Rectangular	475	595	0.7483	30	20.1	0.373	0.656	0.205
Circular	d =600		0.8500	30	20.1	1.000	1.000	0.296

The interaction curves for the square and rectangular columns given in Fig.9 fall significantly below those of the reference circular column. Under pure compression, the axial strengths of the two square columns with the corner radius of 30 mm and 60 mm, and the rectangular column are only 78%, 81% and 75% of the reference circular column, respectively (Fig.9a). An increase in the corner radius is beneficial in terms of both strength and ductility. Note that a larger aspect ratio (h/b) results in a lower axial strength of the confined column under pure compression, but results in a slightly higher moment capacity (Fig.9a) and curvature ductility (Figs.9b and 9c) in the case that bending is dominant, although this small change is of no interest in a design point of view.

CONCLUSION

This paper has been concerned with the analysis and behaviour of FRP-confined RC circular and rectangular short columns subjected to eccentric loading which produces a combined action of axial load and bending. A parametric study based on a simple stress-strain model for FRP-confined concrete leads to the following conclusions:

(1) The axial strength, moment capacity and curvature ductility of a RC column can be considerably enhanced by using the FRP confinement, and a higher amount of FRP produces a higher degree of the enhancement. In the case of pure bending and FRP jackets with fibres oriented only in the hoop direction, a significant increase in the column ductility with little increase in the moment capacity of the columns results. In this case, the use of longitudinal FRP has to be considered in order to increase the bending moment capacity.

(2) The ultimate axial strain of confined concrete can be higher in a column wrapped with AFRP than in a column wrapped with CFRP, if both FRP wraps provide the same maximum confining pressure. This is because the AFRP has a higher strain capacity than the CFRP. While this increased ultimate strain has no effect on the axial strength and moment capacity of the confined column, it yields a considerable improvement in the curvature ductility of the column.

(3) An increase in the unconfined concrete strength has different effects on the moment capacity of the confined column at axial load levels above and below the axial strength of the unconfined column. An increased unconfined concrete strength reduces the curvature ductility of the column because the ultimate axial strain of confined concrete is reduced without increasing the amount of FRP.

(4) The FRP confinement is much less effective for rectangular columns but an increase in the corner radius is beneficial to both strength and ductility. An increase in the aspect ratio has a negative effect on the axial strength of the FRP-confined column, but may have small beneficial effects on the moment capacity and ductility.

ACKNOWLEDGEMENTS

The authors wish to thank The Hong Kong Polytechnic University for its financial support provided through the Area of Strategic Development (ASD) Scheme for the ASD in Advanced Buildings Technology in a Dense Urban Environment and through postdoctoral fellowships awarded to the third and fourth authors. Special thanks go to Prof. J.G. Teng of The Hong Kong Polytechnic University for offering invaluable advice during the preparation of the paper.

References

Cheng, H.L., Sotelino, E.D., Chen, W.F., 2002. Strength estimation for FRP wrapped reinforced concrete columns. *Steel and Composite Structures*, **2**(1):1-20.

de Lorenzis, L., Tepfers, R., 2002a. Performance Assessment of FRP-confinement Models—Part I: Review of

Experiments and Models. Proceedings of the First International Conference on Advanced Polymer Composites for Structural Applications in Construction. London, UK, p.251-260.

de Lorenzis, L., Tepfers, R., 2002b. Performance Assessment of FRP-confinement Models—Part II: Comparison of Experiments and Predictions. Proceedings of the First International Conference on Advanced Polymer Composites for Structural Applications in Construction. London, UK, p.261-269.

Hadi, M.N.S., 2007. Behaviour of FRP strengthened concrete columns under eccentric compression loading. *Composite Structures*, **77**(1):92-96. [doi:10.1016/j.compstruct.2005.06.007]

Harajli, M.H., 2006. Axial stress-strain relationship for FRP confined circular and rectangular concrete columns. *Cement & Concrete Composites*, **28**(10):938-948. [doi:10.1016/j.cemconcomp.2006.07.005]

Lam, L., Teng, J.G., 2003a. Design-oriented stress-strain model for FRP-confined concrete. *Construction and Building Materials*, **17**(6-7):471-489. [doi:10.1016/S0950-0618(03)00045-X]

Lam, L., Teng, J.G., 2003b. Design-oriented stress-strain model for FRP-confined concrete in rectangular columns. *Journal of Reinforced Plastics and Composites*, **22**(13):1149-1186. [doi:10.1177/0731684403035429]

Mander, J.B., Priestley, M.J.N., Park, R., 1988. Theoretical stress-strain model for confined concrete. *Journal of Structural Engineering, ASCE*, **114**(8):1804-1826.

Mirmiran, A., Singhvi, A., 2001. Discussion: 'FRP-confined concrete model'. *Journal of Composites for Construction, ASCE*, **5**(1):62-63. [doi:10.1061/(ASCE)1090-0268(2001)5:1(62)]

Mirmiran, A., Naguib, W., Shahawy, M., 2000. Principle and analysis of concrete filled composite tubes. *Journal of Advanced Materials*, **32**(4):16-23.

Monti, G., Nistico, N., Santini, S., 2001. Design of FRP jackets for upgrade of circular bridge piers. *Journal of Composites for Construction, ASCE*, **5**(2):94-101. [doi:10.1061/(ASCE)1090-0268(2001)5:2(94)]

Saadatmanesh, H., Ehsani, M.R., Li, M.W., 1994. Strength and ductility of concrete columns externally reinforced with fiber composites straps. *ACI Structural Journal*, **91**(4):434-447.

Saadatmanesh, H., Ehsani, M.R., Jin, L., 1996. Seismic strengthening of circular bridge pier models with fiber composites. *ACI Structural Journal*, **93**(6):639-647.

Samaan, M., Mirmiran, A., Shahawy, M., 1998. Model of concrete confined by fiber composite. *Journal of Structural Engineering, ASCE*, **124**(9):1025-1031. [doi:10.1061/(ASCE)0733-9445(1998)124:9(1025)]

Seible, F., Priestley, M.J.N., Hegemier, G.A., Innamorato, D., 1997. Seismic retrofit of RC columns with continuous carbon fiber jackets. *Journal of Composites for Construction, ASCE*, **1**(2):52-62. [doi:10.1061/(ASCE)1090-0268(1997)1:2(52)]

Spoelstra, M.R., Monti, G., 1999. FRP-confined concrete model. *Journal of Composites for Construction, ASCE*, **3**(3):143-150. [doi:10.1061/(ASCE)1090-0268(1999)3:3(143)]

Teng, J.G., Chen, J.F., Smith, S.T., Lam, L., 2002. FRP-Strengthened RC Structures. John Wiley and Sons, UK, p.238.

Xiao, Y., Wu, H., Martin, G.R., 1999. Prefabricated composite jacketing of RC columns for enhanced shear strength. *Journal of Structural Engineering, ASCE*, **125**(3):255-264. [doi:10.1061/(ASCE)0733-9445(1999)125:3(255)]

Youssef, M.N., Feng, M.Q., Mosallam, A.S., 2007. Stress-strain model for concrete confined by FRP composites. *Composites Part B: Engineering*, **38**(5-6):614-628. [doi:10.1016/j.compositesb.2006.07.020]